Chemical Science

ROYAL SOCIETY OF CHEMISTRY

EDGE ARTICLE

View Article Online
View Journal | View Issue

Cite this: *Chem. Sci.*, 2021, **12**, 13572

All publication charges for this article have been paid for by the Royal Society of Chemistry

Depolymerization of supramolecular polymers by a covalent reaction; transforming an intercalator into a sequestrator†

Kasper M. Vonk, E. W. Meijer and Ghislaine Vantomme *

Received 17th August 2021
Accepted 22nd September 2021

DOI: 10.1039/d1sc04545h

rsc.li/chemical-science

Controlling the reciprocity between chemical reactivity and supramolecular structure is a topic of great interest in the emergence of molecular complexity. In this work, we investigate the effect of a covalent reaction as a trigger to depolymerize a supramolecular assembly. We focus on the impact of an *in situ* thiol–ene reaction on the (co)polymerization of three derivatives of benzene-1,3,5-tricarboxamide (BTA) monomers functionalized with cysteine, hexylcysteine, and alkyl side chains: **Cys-BTA**, **HexCys-BTA**, and **a-BTA**. Long supramolecular polymers of **Cys-BTA** can be depolymerized into short dimeric aggregates of **HexCys-BTA** *via* the *in situ* thiol–ene reaction. Analysis of the system by time-resolved spectroscopy and light scattering unravels the fast dynamicity of the structures and the mechanism of depolymerization. Moreover, by intercalating the reactive **Cys-BTA** monomer into an unreactive inert polymer, the *in situ* thiol–ene reaction transforms the intercalator into a sequestrator and induces the depolymerization of the unreactive polymer. This work shows that the implementation of reactivity into supramolecular assemblies enables temporal control of depolymerization processes, which can bring us one step closer to understanding the interplay between non-covalent and covalent chemistry.

Introduction

In the field of supramolecular polymerisation, much progress has been achieved in understanding the assembly properties and pathway selection of the products obtained.[1,2] Often the construction of these structures is divided into two unconnected steps: first the covalent synthesis of the building blocks followed by the study of their self-assembly properties in solution. In contrast, concomitant covalent modifications of structures held together by non-covalent interactions are widespread in living systems.[3] This connection between biological materials with chemical reaction networks results in the spatio-temporal control needed to sustain the complex functions of life. A fascinating example on how nature controls dynamic supramolecular systems by incorporating covalent reactions is the dynamic instability of microtubules that governs their cyclic growth and shrinkage.[4,5] Microtubules consist of α/β-tubulin molecules that can polymerize into long fibres by incorporation of guanosine di- or triphosphate (GDP or GTP) on the growing end of the tubules. Hydrolysis of GTP into GDP destabilizes the fibre and triggers depolymerization. Addition of new GTP to the stack stabilizes the fibre and initiates the growth cycle again.[4,5] Integration of this fine level of control and precision over aggregation mechanisms by combining covalent and non-covalent synthesis would be of great interest to tackle the challenge of recyclability of supramolecular materials. Inspired by these systems, the interplay between structure and reactivity can serve as a stepping stone towards the design of functional and life-like 1D supramolecular materials.[6–8]

Recently, chemists have combined covalent and non-covalent synthesis for the construction of complex molecular systems.[9] Methods to construct these complex systems require implementing chemical reactivity into synthetic supramolecular assemblies. Inclusion of chemical functionality in the assembled building blocks enables *in situ* covalent modification, which induces changes in the structural unit and consequently impacts the assembly properties. In supramolecular polymerization, the lability of the non-covalent interactions makes the structures intrinsically dynamic and sensitive to changes in molecular functionalities and external conditions. Therefore, aside from increase in temperature,[10–13] addition of cosolvent,[14,15] and use of supramolecular additives,[16–19] the modification of structural units by covalent reactions would provide an alternative method to control supramolecular polymerization. Elegant examples have been presented in which adaptation, regulation and replication can be demonstrated by integrating chemical reactions with polymerization processes.[20–24] Complementarily, deepening our understanding on the molecular mechanisms at stake and structure–property relationships is essential as the complexity of molecular systems is ever growing, in particular in the

Institute for Complex Molecular Systems, Laboratory of Macromolecular and Organic Chemistry, Eindhoven University of Technology, P.O. Box 513, 5600 MB Eindhoven, The Netherlands. E-mail: g.vantomme@tue.nl

† Electronic supplementary information (ESI) available. See DOI: 10.1039/d1sc04545h

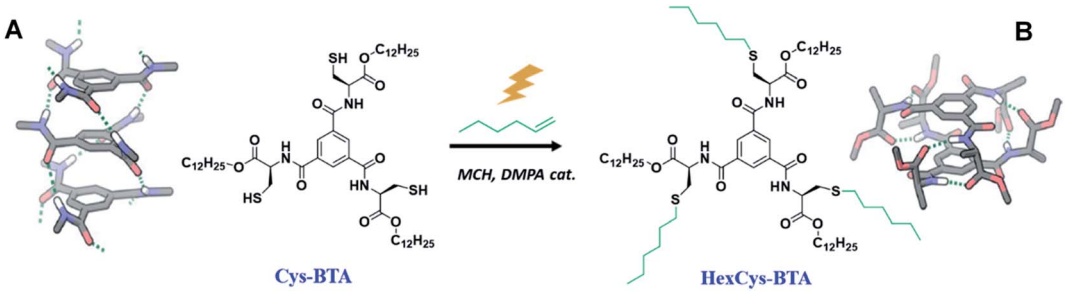

Scheme 1 An overview of the structures of benzene-1,3,5-tricarboxamides **Cys-BTA** and **HexCys-BTA** and the transformation induced by the thiol–ene reaction. (A) The molecular structure of the helical stack formed by **Cys-BTA** derived from X-ray data[31] and (B) the dimeric hydrogen-bonded structure formed by **HexCys-BTA** derived from DFT calculations.[25]

cooperative supramolecular polymerization of reactive multi-component systems.

The assembly of benzene-1,3,5-tricarboxamides derivatised with amino-ester side chains (ester-BTAs) has been reported in great details.[25,26] Studies have demonstrated that the nature of the side chains dramatically influences the structure, length, and mechanism of formation of the aggregates. Ester-BTAs are known for their ability to self-assemble into helical stacks in apolar solvent by formation of an intermolecular three-fold hydrogen bonding between the amides or into dimeric structures by six-fold hydrogen bonding of the ester carbonyls depending on the nature of the side chains, the concentration and the temperature of the solutions (Scheme 1).[25] Recently, these chiral ester-BTA have been shown to intercalate into achiral assemblies and generate homochiral helices, indicating the effectiveness of ester-BTAs in steering the co-assembly process.[27–30]

Here, we report on the controlled depolymerization of supramolecular 1D polymers into well-defined dimers triggered by a covalent reaction on the side chains of the monomer. For the purpose of this study, we selected **Cys-BTA**, a monomer of BTA derived from cysteine with a thiol containing residue. In the assembly of this monomer, a morphological change from stacks to dimeric species is induced by performing a covalent reaction on these reactive thiol groups. The changes in both the hydrogen bond pattern and the size of the aggregates were analysed by spectroscopic and light scattering techniques to follow the kinetics of the reaction. A detailed analysis was conducted to understand how the differences in molecular structure of the monomers (reagents and products) and the kinetics of the thiol–ene reaction affect the depolymerization and the overall mechanism of the process. Moreover, an unreactive achiral alkyl-BTA monomer copolymerized with a **Cys-BTA** additive was also depolymerized upon performing the thiol–ene reaction on **Cys-BTA**. These results demonstrate how an unreactive monomer in a multi-component system can be depolymerized by a covalent reaction through competitive interactions with a reactive sequestrator.

Results and discussion

Chiral **Cys-BTA** and **HexCys-BTA** were synthesized in four and five steps with 57% and 31% yield respectively, starting from the commercial protected *N*-Fmoc-*S*-trityl-cysteine amino acid and 1,3,5-benzenetricarbonyltrichloride (see ESI† for details). The synthesis starts by the esterification of the commercial *N*-Fmoc-*S*-trityl-cysteine amino acid with 1-dodecanol. The optically pure *N*-Fmoc-*S*-trityl-cysteine dodecyl ester is subsequently deprotected by removal of the Fmoc group and reacted with 1,3,5-benzenetricarbonyltrichloride. The removal of the trityl protective group yields the **Cys-BTA**, as a gum-like solid. Finally, **HexCys-BTA** was synthesized by a photo-initiated thiol–ene reaction on **Cys-BTA**. All compounds were purified by column chromatography and fully characterized by ^{1}H and ^{13}C NMR spectroscopy and MALDI (Fig. S1–S6†).

Homoaggregation of Cys-BTA and dimerization of HexCys-BTA

We first investigated the homopolymerization properties of **Cys-BTA** and **HexCys-BTA** in both bulk and apolar solution. Measurements in bulk show that both **Cys-BTA** and **HexCys-BTA** assemble into helical stacks (Table 1, Fig. S7 and S8†). In solution, **Cys-BTA** forms both long supramolecular polymers and dimers depending on the concentration, whereas **HexCys-BTA** only assembles into dimers (Table 1). The details of the combined NMR, IR, UV and CD spectroscopy analysis of the assembly in solution are presented in the paragraphs below.

Fig. 1 shows that the IR spectrum of **Cys-BTA** in 1 mM methylcyclohexane (MCH) solution displays an N–H stretch at about $\approx$3229 cm^{-1}, the unbonded ester at $\approx$1748 cm^{-1}, C=O amide I at $\approx$1644 cm^{-1}, and the amide II at $\approx$1558 cm^{-1}. The unbonded ester and bonded carbonyl of the amide suggests the presence of one-dimensional polymers stabilized by helically ordered, intermolecular hydrogen-bonds. In contrast, the IR spectrum of **HexCys-BTA** presents vibrations for the NH stretch at $\approx$3388 cm^{-1}, the bonded ester at $\approx$1737 cm^{-1}, the free amide I at $\approx$1675 cm^{-1}, and the free amide II at $\approx$1527 cm^{-1}. In this case, the bands imply the presence of dimers with intermolecular hydrogen bond formation between the N–H protons and the ester carbonyls. The formation of helically-ordered polymers and dimeric structures for **Cys-BTA** and **HexCys-BTA**, respectively, are in line with previous studies on the aggregation of these ester-BTAs.[25] From the IR data, the critical concentration (c*) for polymerization of **Cys-BTA** was determined to be approximately 0.150 mM in MCH at 20 °C

Table 1 Assembly properties of **Cys-BTA** and **HexCys-BTA**

	Assembly in bulk		Assembly in solution		
	Structure	T_c [a]	Structure	c^* [b]	Viscosity
Cys-BTA	Stacks	170 °C	Dimers + stacks	0.150 mM	Viscous
HexCys-BTA	Stacks	130 °C	Dimers	—[c]	Fluid

[a] Crystallization transition temperature (T_c) determined with DSC using a cooling rate of 5 K min^{-1}. [b] The critical concentration (c^*) from which stacks predominate over dimers in MCH solution investigated at 20 °C. [c] No transition between dimers and stacks have been observed in the range of concentrations 0.05–10 mM at 20 °C.

(Fig. S9†), below which the dominant species shifted from the helical assemblies to the dimers. **HexCys-BTA** remained in its dimeric form irrespective of concentration, indicating that the steric hindrance posed by the hexyl group prevents further aggregation even at high concentrations.

CD spectroscopy provides further evidence for the existence of the assemblies determined by IR spectroscopy. Fig. 1 shows that at 50 μM in MCH, both **Cys-BTA** (dashed blue trace) and **HexCys-BTA** (dashed orange trace) display the chiroptical signatures of dimers (maxima at $\lambda^- = 205$ nm, $\lambda^+ = 225$ nm, and $\lambda^- = 255$ nm). While no change in the shape of the CD spectrum of **HexCys-BTA** (orange trace) occurred upon increasing the concentration to 0.2 mM, the spectrum of **Cys-BTA** (blue trace) shows both a shift for the maximum $\lambda^+ = 225$ nm to 220 nm and the disappearance of the minimum at $\lambda^- = 255$ nm. This transition indicates the formation of helical stacks at a concentration of 0.2 mM. Moreover, NMR spectroscopy of 5 mM MCH solution of **Cys-BTA** (Fig. S10A†) confirms the aggregation into large assemblies as only broad signals are observed and no signals related to protons of the BTA core are visible. In contrast, 5 mM MCH solution of **HexCys-BTA** shows well-resolved signals, confirming the formation of well-defined dimers because of the diastereotopicity of the H_1 and H_2 protons in the ester-bonded dimer (Fig. S10B†).[25,32] Additionally, in the more polar solvent $CHCl_3$, a single signal is observed at 4.2 ppm indicating the presence of only monomers in solution (Fig. S10C†). In MCH, splitting of this same signal at 4.2 ppm occurs which is characteristic of six-folded hydrogen bonding. Additionally, fitting of the scattering curves to a cylindrical model with a fixed radius of 6 nm also provided us with an approximate length of 180 nm for the helical **Cys-BTA** assembly (Fig. S11†).[33] Variable temperature measurement in CD also revealed that at a concentration of 200 μM in MCH, the homodimer of **HexCys-BTA** remains stable between 10 °C and 90 °C, whereas the CD spectrum of **Cys-BTA** at the same concentration shifts from a helical to a dimeric shape around 40 °C (Fig. S12†). The lack of isodichroic point for **Cys-BTA** further supports the presence of multiple species (monomers, short aggregates and stacks) co-existing in solution.[24] The relatively low temperature required for this change in morphology is indicative of the instability of the helical assembly at this specific concentration (Fig. S12†).

To understand the mechanism of dimerization in more detail, we explored the possibility of heteroaggregates formation between **HexCys-BTA** and **Cys-BTA** (Fig. 2). This study is similar to previously reported results on the mixing of dimeric ester-BTA and polymeric alkyl-BTA.[27,33] IR and CD data point to the exclusive formation of heterodimers between **HexCys-BTA** and **Cys-BTA** above 50 mol% of **HexCys-BTA** (Fig. 2). Decrease of the ratio of **HexCys-BTA** below 50 mol% leads to the co-existence of heterodimers, homodimers of **HexCys-BTA** and **Cys-BTA** dominated fibres with intercalated **HexCys-BTA**. In details, the comparison of the IR spectra of 1 mM MCH solutions of **Cys-BTA**/**HexCys-BTA** mixtures (blue to orange traces in Fig. 2B)

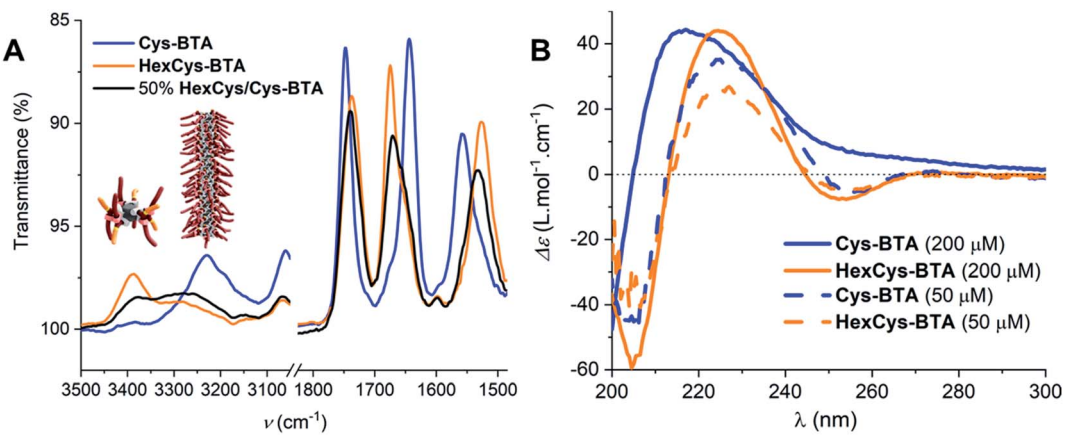

Fig. 1 (A) IR spectra of **Cys-BTA** (blue), **HexCys-BTA** (orange), and 50 mol% **Cys-BTA**/**HexCys-BTA** (black) at 1 mM in MCH at 20 °C. (B) CD spectra of **Cys-BTA** (blue) and **HexCys-BTA** (orange) at 50 μM and 200 μM in MCH at 20 °C.

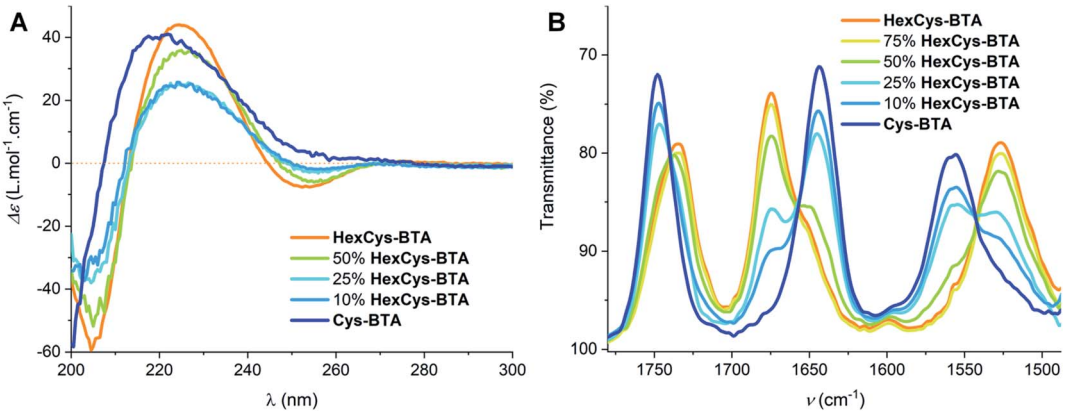

Fig. 2 (A) CD spectra of different ratios of **HexCys-BTA** and **Cys-BTA** (percentages are given in moles of **HexCys-BTA** mixed with **Cys-BTA** in solution) at a total concentration of 0.2 mM in MCH at 20 °C. (B) The IR spectra of different ratios of **Cys-BTA**/**HexCys-BTA** mixtures at 1 mM in MCH at 20 °C.

shows a transition from helical stacks to dimeric species above 50 mol% of **HexCys-BTA** indicating the interaction between the two monomers. Furthermore, it shows that addition of 50 mol% of **HexCys-BTA** is sufficient to depolymerize the helical assembly by formation of heterodimers. Even at 10 mol% of **HexCys-BTA**, a small band at 1675 cm^{-1} can be observed, which corresponds to the formation of dimers and thus indicates the ability of **HexCys-BTA** to act as a sequestrator by stabilizing the free **Cys-BTA** monomers.[24] The CD spectra of the **Cys-BTA**/**HexCys-BTA** mixtures show a similar trend where a small negative minimum at $\lambda_{min} = 255$ nm can be observed, which indicates the presence of dimers (Fig. 2A).

Supramolecular depolymerization of Cys-BTA 1D fibres into HexCys-BTA dimers upon covalent reaction

The difference in the aggregation properties of the **Cys-BTA** helical polymers and **HexCys-BTA** dimers prompted us to investigate the *in situ* depolymerization of **Cys-BTA** aggregates over the course of a thiol–ene reaction yielding dimers of **HexCys-BTA** (Scheme 2). The thiol–ene reaction was selected due to its compatibility with both the apolar solvent and temperature range for the existence of the helical BTA stacks.

To elucidate in detail the efficiency of the *in situ* depolymerization, we conducted a series of experiments analysed by NMR, IR, CD, and static light scattering (SLS) (Fig. 3–5). Addition of 0.3 eq. of catalyst 2,2-dimethoxy-2-phenyl acetophenone (DMPA) and 3 eq. of 1-hexene (stoichiometric amount) to a solution of **Cys-BTA** (MCH, 1 mM) and subsequent irradiation with UV light for 10 minutes, results in a shift in the CD signals from the helical assembly to the chiroptical signatures of dimers (Fig. 3A). This observation suggests the *in situ* conversion of **Cys-BTA** to **HexCys-BTA**. ^{1}H-NMR spectroscopy confirms this *in situ* conversion, as new and sharper signals corresponding to the formation of **HexCys-BTA** emerge in the spectrum (Fig. S13C†) attributed to short defined aggregates of **HexCys-BTA** (Fig. S13D†).

Kinetics experiments give valuable information on the mechanism of the depolymerization. Interestingly, by combining different characterization techniques, both changes

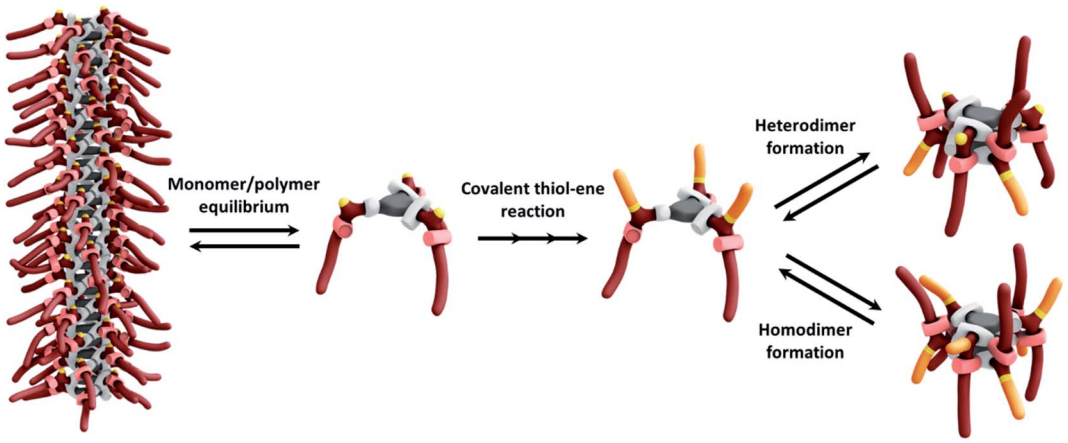

Scheme 2 Schematic overview of the supramolecular depolymerization of **Cys-BTA** polymers by thiol–ene reaction on the side chains of **Cys-BTA**. In solution, the monomer and polymer are in equilibrium and occurrence of the covalent thiol–ene reaction decreases the **Cys-BTA** monomer concentration and forms **HexCys-BTA**, which favours the formation of homo- and heterodimers.

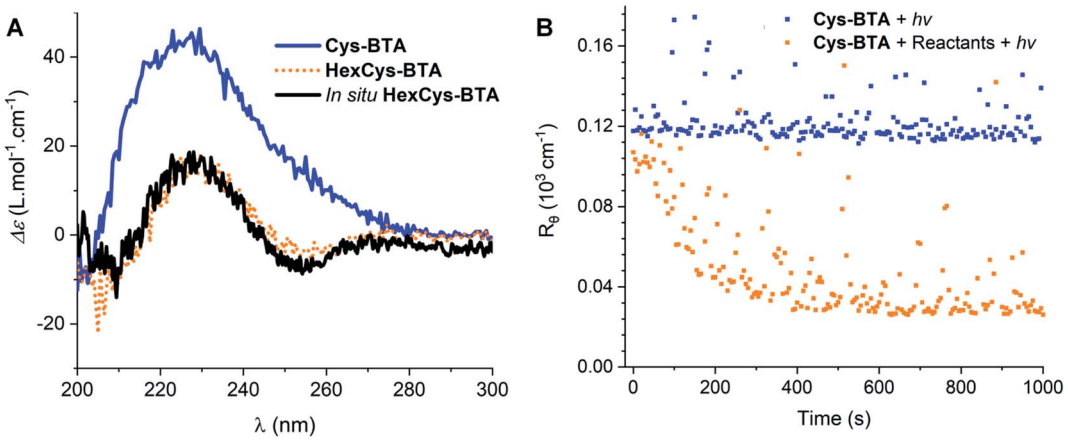

Fig. 3 (A) CD spectra of **Cys-BTA** (blue), **HexCys-BTA** (orange) and the *in situ* formed **HexCys-BTA** (black) after 20 minutes exposure to UV light ($\lambda = 365$ nm, 70 mW cm^{-2}) measured at 1 mM in MCH at 20 °C. (B) SLS data showing the change in particle size over UV irradiation time ($\lambda = 365$ nm, 70 mW cm^{-2}) of the mixture of **Cys-BTA** with reactants (orange) and without reactants (blue) measured at 0.5 mM in MCH at 20 °C.

in structural morphologies and chemical conversion can be followed over time at various concentrations. Time-resolved IR spectroscopy was used to provide insights into the changes from polymers to dimers and chemical conversion over time (Fig. 4), while kinetics of the reaction followed by SLS (Fig. 3B) and CD (Fig. S14†) gave the change in the aggregate size and morphology, respectively. Over 20 minutes irradiation of a 1 mM MCH solution containing **Cys-BTA**, 1-hexene (3 eq.), and DMPA (0.3 eq.), a shift in the distinctive bands of the NH stretch (from ≈3240 cm^{-1} to ≈3389 cm^{-1}) and the three carbonyl bands (between 1500 and 1800 cm^{-1}) was observed in IR spectroscopy and attributed to the change in hydrogen bonding pattern from helical assemblies to dimers (Fig. 4). Moreover, the band at $\nu = 2559$ cm^{-1}, distinctive of the unreacted thiol moiety, allows to follow the quantitative conversion of free thiol over 20 minutes (Fig. 4). Kinetics of the conversion of the thiol and the loss of polymers show a similar shape (Fig. S15†). However, the disappearance of these polymers exhibits a lag time (about 2 minutes) in comparison to the thiol conversion, indicating that the thiol–ene reaction does not immediately result in a change of the assembly. The presence of such a lag time was already noted on the kinetics of "sergeant and soldiers" experiments with BTA, which is attributed to the exchange dynamics between the two components.[34] The depolymerization of **Cys-BTA** elongated structures over the course of the thiol–ene reaction was also confirmed by SLS (Fig. 3B and S11†). Without the catalyst and 1-hexene, no change in size of the aggregates was observed upon UV irradiation, whereas when these reactants are present a decrease in fibre length was observed after 5 minutes, until the fibres disappear. Combined with the fact that the thiol–ene reaction, unlike most radical reactions, is not affected by oxygen in the air,[35] it indicates that the observed changes over time are the result of the thiol–ene reaction between the terminal thiol unit on **Cys-BTA** side chain and the double bond of hexene to form **HexCys-BTA**. Conversion of **Cys-BTA** into **HexCys-BTA** decreases the free monomer concentration of **Cys-BTA** and induces the formation of heterodimers **Cys-BTA**/**HexCys-BTA**, which therefore pushes the thermodynamic equilibrium of formation of **Cys-BTA** polymers towards depolymerization.

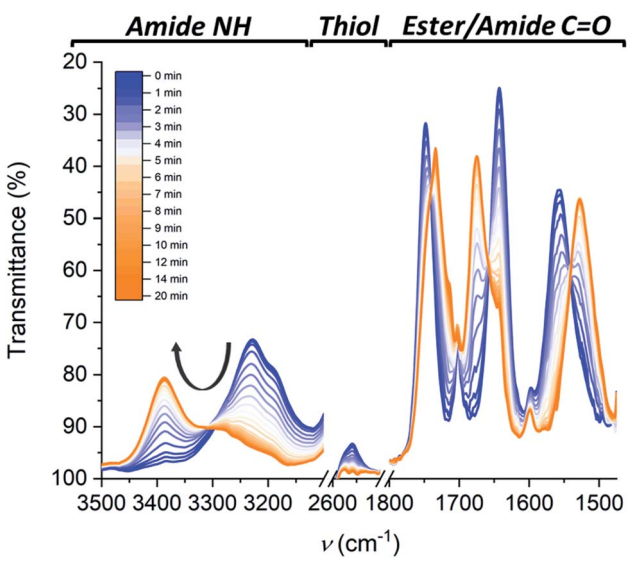

Fig. 4 The change in FT-IR spectra over time following the thiol–ene reaction in the **Cys-BTA** solution from the characteristic bands of polymers (blue) to the bands of dimers (orange). The spectra are taken at a concentration of 10 mM in MCH at 20 °C under UV light irradiation ($\lambda = 365$ nm, 70 mW cm^{-2}). Each spectrum was taken at an interval of 30 seconds from the blue to the orange traces over the course of 20 minutes.

The normalized kinetic profiles followed at different concentrations between the different techniques were compared (ranging from 0.2 to 10 mM MCH solutions from CD, IR, and SLS kinetic data, Fig. 5A) and no major difference in kinetics was observed. The data were fitted to first order kinetics, which is in correspondence with the usual dependence on the thiol concentration for the thiol–ene reaction between a large variety of thiol/alkene pairs.[36,37] Due to the relatively high light intensities used in this study (70 W cm^{-2}), we assume that

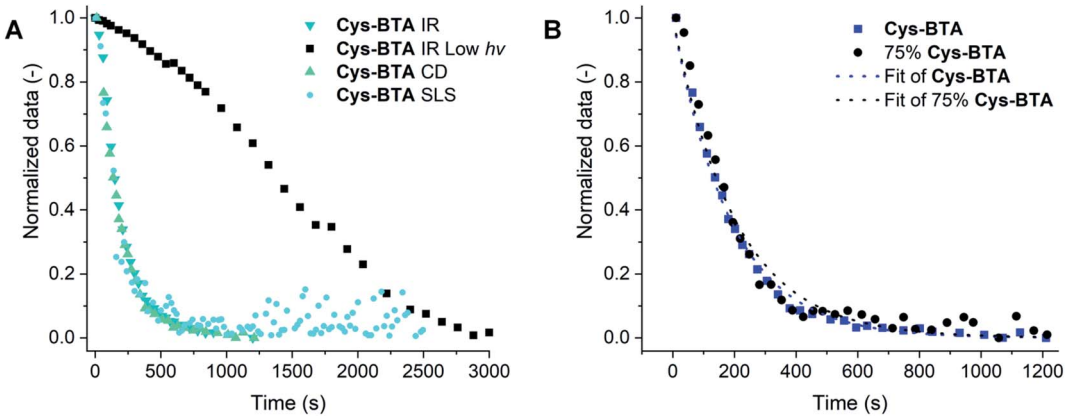

Fig. 5 (A) The normalized kinetics of the IR ($\nu = 2559$ cm^{-1}, 10 mM in MCH, 70 mW cm^{-2} or 2 mM in MCH, 7 mW cm^{-2} for IR low light intensity), CD (at $\lambda = 214$ nm, 0.2 mM in MCH), and SLS data (0.5 mM in MCH) showing the change in signal intensities over time during UV irradiation at 20 °C. Fitting of the data is given in Fig. S16.† (B) The normalized data of the change in CD intensity at $\lambda = 214$ nm during the thiol–ene reaction performed on pure **Cys-BTA** (blue) and on the 3/1 **Cys-BTA**/**a-BTA** mixture (75 mol% **Cys-BTA**, black) at 0.2 mM in MCH at 20 °C. The dotted lines are the fitted data to first order kinetics (see ESI†).

the concentration of free radicals reaches its steady state quickly and ultimately be of negligent impact. Furthermore, we assume that thus the chain transfer step (movement of the radical from the formed sulfide to a new thiol group) can be considered as the rate-limiting step.[38,39] When the reaction is performed with low light intensity (365 nm, ~7 mW cm^{-2}), and followed by IR, the kinetics of thiol conversion and polymers disappearance overlap with approximately 50% conversion of the thiol after 23 minutes of irradiation corresponding to 50 mol% of the polymer disappearance (Fig. S17†). This result is surprising because the presence of 50 mol% **HexCys-BTA** with **Cys-BTA** normally results in the formation of heterodimers. We attribute this difference to the formation of asymmetric mono- and di-substituted **Cys-BTA**, which are less bulky than **HexCys-BTA** and could therefore more easily intercalate into the **Cys-BTA** stacks.

The depolymerization of the supramolecular aggregates can also be probed on a macroscopic scale. The ability of BTAs with alkyl side chains to form gels in apolar solvent is a well-known feature.[40] The addition of catalyst and 3 eq. of hexene to a gel of **Cys-BTA** (40 mM in MCH) and irradiation with UV light resulted in an immediate loss in viscosity and the self-supporting properties of the gel (Fig. S18†). This loss of gel property is attributed to the *in situ* thiol–ene reaction, which initiates the covalent modification of **Cys-BTA** to form **HexCys-BTA** and results in the disassembly of the helical structures into dimers.

Depolymerization of inactive polymers by competitive interactions

Going further, after establishing the depolymerization of **Cys-BTA** polymers into dimers *via* the thiol–ene reaction, we investigated how this covalent modification can influence the polymerization of an inert monomer copolymerized with **Cys-BTA**. Indeed, the polymerization of achiral alkyl **a-BTA** can be controlled by copolymerization with a second component, such as a chain capper or a sequestrator.[18,33,41] Previous work from our group[19] has shown that copolymerizing the inert **a-BTA** polymers with a small amount of responsive chain capper can lead to a large decrease in polymer length. Because of this sensitivity of supramolecular systems to additives and changes in molecular structures, we hypothesized that the covalent transformation of **Cys-BTA** into **HexCys-BTA** should affect the overall cooperative assembly of the inactive monomer **a-BTA**. In "sergeant-and-soldiers" experiments[34] between the soldiers **a-BTA** and either the sergeants **Cys-BTA** or **HexCys-BTA**, two different trends are observed. The presence of 4 mol% of either **Cys-BTA** or **HexCys-BTA** showed a helical bias in stacking of **a-BTA**, which points to the intercalation of these monomers into the **a-BTA** stacks (Fig. S19†). However, in a second trend at higher ratio of sergeants (>50 mol%), while **Cys-BTA** still intercalates into **a-BTA** polymers, in the case of **HexCys-BTA** a sequestration by formation of heterodimers of **HexCys-BTA**/**a-BTA** and homodimers of **HexCys-BTA** is obtained (Fig. S19–S21†). As a result, the *in situ* thiol–ene reaction of a 3/1 **Cys-BTA**/**a-BTA** mixture shows conversion from mainly polymers to mainly **HexCys-BTA**/**a-BTA** heterodimers, as followed by observing the decrease of the helical aggregates CD signal over irradiation time (Fig. 5B). Comparison of the decay in CD intensity of the helical aggregates for the pure **Cys-BTA** and the 3/1 **Cys-BTA**/**a-BTA** mixture display similarly shaped curves, with reaction rate constants of approximately $k \approx 5 \times 10^{-3}$ s^{-1} underlying the high dynamicity of this system. This demonstrates how an unreactive monomer in a multi-component system can be depolymerized by a covalent reaction through competitive interactions with a reactive sequestrator.

Conclusions

In conclusion, we have been able to induce depolymerization of supramolecular fibres by introducing covalent synthesis into the system. By performing the covalent reaction on the side chain of the monomer, the hydrogen bond pattern for assembly

changes from formation of cooperative polymers to short, ordered aggregates, which was followed by spectroscopy and light scattering. The depolymerization of the supramolecular fibres into ordered dimers was achieved by the use of a photo-initiated thiol–ene reaction, which allowed for additional temporal control over the reaction. The results indicate that supramolecular systems are sensitive to small alterations in molecular structure, as small changes in steric hindrance and polarity have been shown to have a large effect on morphologies. Detailed analysis has shown that usage of 10% of the modified BTA can induce partial depolymerization of the helical assembly, but optimally 50% is used to depolymerize the assembly into heterodimers. These ester-BTAs can also be used to induce depolymerization of inactive polymer, which shows that stabilization of the inactive monomer by competitive interactions with a sequestrator plays an important role in the depolymerization process. Application of these types of covalent steps on non-covalent assemblies creates a new set of tools for exploring the world of supramolecular total synthesis and come closer to the complexity of natural supramolecular systems.

Data availability

All experimental procedures characterization data and Fig. S1–S21 can be found in the ESI.†

Author contributions

K. M. V. performed the experiments. K. M. V., E. W. M. and G. V. interpreted the results. G. V. supervised the overall research. All authors contributed to the writing of the manuscript.

Conflicts of interest

There are no conflicts to declare.

Acknowledgements

This work was financially supported by The Netherlands Organization for Scientific Research (NWO-VENI Grant 722.017.003), the Dutch Ministry of Education, Culture and Science (Gravity Program 024.001.035) and the European Research Council (H2020-EU.1.1., SYNMAT project, ID 788618). The ICMS Animation Studio is acknowledged for providing the artwork.

References

1 T. Aida, E. W. Meijer and S. I. Stupp, *Sci. 80*, 2012, **335**, 813–817.
2 M. Hartlieb, E. D. H. Mansfield and S. Perrier, *Polym. Chem.*, 2020, **11**, 1083–1110.
3 C. T. Walsh, *Posttranslational Modification of Proteins*, Roberts & Company Publishers, Greenwood Village, 2006.
4 M. Igaev and H. Grubmüller, *PLoS Comput. Biol.*, 2020, **16**, e1008132.
5 T. Mitchison and M. Kirschner, *Nature*, 1984, **312**, 237–242.
6 A. R. Studart, *Angew. Chem., Int. Ed.*, 2015, **54**, 3400–3416.
7 N. Huebsch and D. J. Mooney, *Nature*, 2009, **462**, 426–432.
8 P. Fratzl and R. Weinkamer, *Prog. Mater. Sci.*, 2007, **52**, 1263–1334.
9 T. Schnitzer and G. Vantomme, *ACS Cent. Sci.*, 2020, **6**, 2060–2070.
10 P. Besenius, G. Portale, P. H. H. Bomans, H. M. Janssen, A. R. A. Palmans and E. W. Meijer, *Proc. Natl. Acad. Sci. U. S. A.*, 2010, **107**, 17888–17893.
11 D. D. Prabhu, K. Aratsu, Y. Kitamoto, H. Ouchi, T. Ohba, M. J. Hollamby, N. Shimizu, H. Takagi, R. Haruki, S. Adachi and S. Yagai, *Sci. Adv.*, 2018, **4**, 8466.
12 J. Matern, Y. Dorca, L. Sánchez and G. Fernández, *Angew. Chem., Int. Ed.*, 2019, **58**, 16730–16740.
13 H. Gao, L. Gao, J. Lin, Y. Lu, L. Wang, C. Cai and X. Tian, *Macromolecules*, 2020, **53**, 3571–3579.
14 R. P. M. Lafleur, X. Lou, G. M. Pavan, A. R. A. Palmans and E. W. Meijer, *Chem. Sci.*, 2018, **9**, 6199–6209.
15 P. A. Korevaar, C. Schaefer, T. F. A. De Greef and E. W. Meijer, *J. Am. Chem. Soc.*, 2012, **134**, 13482–13491.
16 F. Lortie, S. Boileau, L. Bouteiller, C. Chassenieux and F. Lauprêtre, *Macromolecules*, 2005, **38**, 5283–5287.
17 S. H. Jung, D. Bochicchio, G. M. Pavan, M. Takeuchi and K. Sugiyasu, *J. Am. Chem. Soc.*, 2018, **140**, 10570–10577.
18 G. M. ter Huurne, P. Chidchob, A. Long, A. Martinez, A. R. A. Palmans and G. Vantomme, *Chem. – Eur. J.*, 2020, **26**, 9964–9970.
19 E. Weyandt, G. M. Ter Huurne, G. Vantomme, A. J. Markvoort, A. R. A. Palmans and E. W. Meijer, *J. Am. Chem. Soc.*, 2020, **142**, 6295–6303.
20 G. Monreal Santiago, K. Liu, W. R. Browne and S. Otto, *Nat. Chem.*, 2020, **12**, 603–607.
21 J. Boekhoven, W. E. Hendriksen, G. J. M. Koper, R. Eelkema and J. H. Van Esch, *Sci. 80*, 2015, **349**, 1075–1079.
22 S. Dhiman, A. Jain and S. J. George, *Angew. Chem., Int. Ed.*, 2017, **56**, 1329–1333.
23 D. Núñez-Villanueva and C. A. Hunter, *Acc. Chem. Res.*, 2021, **54**, 1298–1306.
24 N. Singh, B. Lainer, G. J. M. Formon, S. De Piccoli and T. M. Hermans, *J. Am. Chem. Soc.*, 2020, **142**, 4083–4087.
25 A. Desmarchelier, B. G. Alvarenga, X. Caumes, L. Dubreucq, C. Troufflard, M. Tessier, N. Vanthuyne, J. Idé, T. Maistriaux, D. Beljonne, P. Brocorens, R. Lazzaroni, M. Raynal and L. Bouteiller, *Soft Matter*, 2016, **12**, 7824–7838.
26 M. Raynal, Y. Li, C. Troufflard, C. Przybylski, G. Gontard, T. Maistriaux, J. Idé, R. Lazzaroni, L. Bouteiller and P. Brocorens, *Phys. Chem. Chem. Phys.*, 2021, **23**, 5207–5221.
27 M. A. Martínez-Aguirre, Y. Li, N. Vanthuyne, L. Bouteiller and M. Raynal, *Angew. Chem., Int. Ed.*, 2021, **60**, 4183–4191.
28 A. Desmarchelier, X. Caumes, M. Raynal, A. Vidal-Ferran, P. W. N. M. Van Leeuwen and L. Bouteiller, *J. Am. Chem. Soc.*, 2016, **138**, 4908–4916.
29 J. M. Zimbron, X. Caumes, Y. Li, C. M. Thomas, M. Raynal and L. Bouteiller, *Angew. Chem., Int. Ed.*, 2017, **56**, 14016–14019.
30 Y. Li, X. Caumes, M. Raynal and L. Bouteiller, *Chem. Commun.*, 2019, **55**, 2162–2165.

31 S. Cantekin, T. F. A. De Greef and A. R. A. Palmans, *Chem. Soc. Rev.*, 2012, **41**, 6125–6137.
32 X. Caumes, A. Baldi, G. Gontard, P. Brocorens, R. Lazzaroni, N. Vanthuyne, C. Troufflard, M. Raynal and L. Bouteiller, *Chem. Commun.*, 2016, **52**, 13369–13372.
33 G. Vantomme, G. M. Ter Huurne, C. Kulkarni, H. M. M. Ten Eikelder, A. J. Markvoort, A. R. A. Palmans and E. W. Meijer, *J. Am. Chem. Soc.*, 2019, **141**, 18278–18285.
34 M. M. J. Smulders, A. P. H. J. Schenning and E. W. Meijer, *J. Am. Chem. Soc.*, 2008, **130**, 606–611.
35 C. E. Hoyle and C. N. Bowman, *Angew. Chem., Int. Ed.*, 2010, **49**, 1540–1573.
36 N. B. Cramer, S. K. Reddy, A. K. O'Brien and C. N. Bowman, *Macromolecules*, 2003, **36**, 7964–7969.
37 B. H. Northrop and R. N. Coffey, *J. Am. Chem. Soc.*, 2012, **134**, 13804–13817.
38 K. W. E. Sy Piecco, A. M. Aboelenen, J. R. Pyle, J. R. Vicente, D. Gautam and J. Chen, *ACS Omega*, 2018, **3**, 14327–14332.
39 M. Claudino, M. Jonsson and M. Johansson, *RSC Adv.*, 2013, **3**, 11021–11034.
40 P. J. M. Stals, J. F. Haveman, A. R. A. Palmans and A. P. H. J. Schenning, *J. Chem. Educ.*, 2009, **86**, 230–233.
41 E. Weyandt, M. F. J. Mabesoone, L. N. J. de Windt, E. W. Meijer, A. R. A. Palmans and G. Vantomme, *Org. Mater.*, 2020, **02**, 129–142.